Journal of NeuroVirology, 14: 229–238, 2008

ISSN: 1355-0284 print / 1538-2443 online
DOI: 10.1080/13550280802093927

informa
healthcare

Microglia are the major cellular source of inducible nitric oxide synthase during experimental herpes encephalitis

Cristina P Marques, Maxim C-J Cheeran, Joseph M Palmquist, Shuxian Hu, and James R Lokensgard

Neuroimmunology Laboratory, Center for Infectious Diseases and Microbiology Translational Research, University of Minnesota Medical School, Minneapolis, Minnesota, USA

Although production of reactive nitrogen and reactive oxygen species (RNS and ROS) is a component of innate defense against viral infection, their overproduction in the brain may also lead to deleterious consequences. To investigate potential immunopathologic roles of oxidative stress during herpes encephalitis, the authors examined the expression kinetics of inducible nitric oxide synthase (iNOS) as well as heme oxygenase-1 (HO-1), a marker of oxidative stress, and evaluated infection-induced oxidative brain damage. Results from these studies showed that both iNOS and HO-1 gene expression were highly elevated in the brain within 7 days post infection (d.p.i.) and remained elevated through 21 d.p.i. Real-time bioluminescence imaging of HO-1 promoter–luciferase transgenic mice confirmed HO-1 promoter activity in the brains of HSV-1-infected animals within 3 d.p.i., which peaked between 5 and 7 d.p.i. Immunohistochemical staining for both 3-nitrotyrosine and 8-hydroxydeoxyguanosine (8-OH-dG), as well as quantitative assessment of 8-isoprostane levels, demonstrated the presence of viral infection-induced oxidative brain damage. In addition, when brain leukocytes obtained from animals with experimental herpes encephalitis were sorted using fluorescence-activated cell sorting (FACS) and the individual cell populations analyzed, CD45(int)/CD11b(+) resident microglia were found to be the major cellular source of iNOS expression. *Journal of NeuroVirology* (2008) **14,** 229–238.

Keywords: HO-1; HSV; iNOS; microglia; oxidative stress

Introduction

Previous studies from our laboratory have shown that vigorous proinflammatory immune responses occur in the brains of herpes simplex virus (HSV)-infected BALB/c mice (Marques *et al*, 2006). The kinetics of these neuroimmune responses, taken together with the kinetics of mortality, suggest that early events in the course of infection play a pivotal role in the progression of experimental herpes encephalitis. We have also previously identified microglial cells as key players in orchestrating these neuroimmune responses (Marques *et al*, 2004). Microglia are a potent cellular source of proinflammatory cytokines, chemokines, and oxidative enzymes in the brain. The production of these innate immune mediators implies both protective as well as potentially detrimental roles during viral brain infection.

Regarded as a critical component of the innate immune response, nitric oxide (NO) has been shown to mediate an array of physiological functions. It is produced endogenously in various cell types by one of three nitric oxide synthases (NOSs; neuronal NOS, endothelial NOS, and inducible NOS [iNOS]). Neurons, endothelial cells, and macrophages are the best characterized producers of NO (Croen, 1993). NO is

Address correspondence to James R. Lokensgard, Neuroimmunology Laboratory, CIDMTR, 3–220 LRB/MTRF, 2001 6th Street S.E., Minneapolis, MN 55455, USA. E-mail: loken006@umn.edu

The authors thank Paul Marker, University of Minnesota Stem Cell Institute, for assistance in sorting brain leukocyte populations. This work was supported by NIH grant MH-066703 and a University of Minnesota Graduate School Doctoral Dissertation Fellowship.

Received 29 February 2008; revised 18 March 2008; accepted 28 March 2008.

known to modulate neuronal function, regulate vasomotor tone, and more pertinent to this study, mediate antimicrobial activity, inflammatory responses, and cytotoxicity (Bredt and Snyder, 1992; Garthwaite, 1991; Moncada *et al*, 1991; Nathan and Hibbs, 1991).

The role of NO during the course of viral brain infection is still unclear. Although NO has been shown to inhibit viral replication, overproduction of this reactive species has also been shown to induce cellular apoptosis and promote tissue damage. Evidence suggests that localized production of NO early during HSV infection may be responsible for decreased pathogenesis (Croen, 1993; Gamba *et al*, 2004; MacLean *et al*, 1998). In contrast, several studies also suggest a pathological role for NO during acute HSV infections. In two different models of HSV-induced disease, it has been reported that treatment of infected animals with the non-selective NOS inhibitor N^{ω}-monomethyl-L-arginine (L-NMMA) resulted in significantly improved survival rates, despite no decrease in viral titers (Adler *et al*, 1997; Fujii *et al*, 1999). Further studies indicate that NO induces proinflammatory responses by stimulating vasodilatation and changes in vascular permeability, which modify leukocyte adhesion and thereby alter immune cell trafficking (Adler *et al*, 1997; Martin *et al*, 1997). Based on such findings, it is likely that brain damage resulting from HSV infection may be partially attributed to host-mediated defense mechanisms, specifically the release of reactive species.

In light of conflicting evidence reported regarding the role of NO during HSV brain infection, it appears that the reported discrepancies may be mediated by alterations in the physiological balance necessary to keep this immune defense mediator from producing deleterious consequences. The immune system has developed mechanisms that regulate the overproduction of NO. The most impressive negative feedback regulator for NO production is the antioxidant enzyme heme oxygenase (HO)-1 (Turcanu *et al*, 1998a, 1998b). Under inflammatory conditions, HO-1 is the rate-limiting enzyme in the degradation of cellular heme, producing equimolar amounts of iron, carbon monoxide (CO), and biliverdin. This cytoprotective anti-inflammatory stress response gene is well known as a marker for oxidative stress and is induced in most cell types by various stimuli such as proinflammatory cytokines, hypoxia, heavy metals, and, most notably, by reactive nitrogen species (RNS) and reactive oxygen species (ROS). Of particular relevance to this study, HO-1 is induced by NO and this induction is also known to inhibit subsequent NO production. The induction of HO-1 mRNA has previously been used as a marker of oxidative stress during HSV-1–induced encephalitis in rat brains following intranasal infection (Fujii et al, 1999). Taken together with mounting evidence that shows HO-1 is a potent mediator of both anti-inflammatory and anti-apoptotic effects, it is plausible that this enzyme plays an important role in protecting NO-secreting cells and the surrounding tissue from oxidative damage (Baranano and Snyder, 2001; Chora *et al*, 2007; Sato *et al*, 2001; Turcanu *et al*, 1998b). Given the intimate relationship between NO and HO-1, we set out to investigate the expression of these mediators in murine brains during experimental herpes encephalitis.

Results

iNOS mRNA induction during herpes encephalitis

We first investigated the kinetics of iNOS mRNA induction in the brains of animals with herpes encephalitis. In these experiments, susceptible BALB/c mice were infected via the intranasal (i.n.) route and the infected brains were collected at 1, 7, 14, and 21 days post infection (d.p.i.). Upon harvesting, the brains were divided into three regions: cortex, subcortex, and cerebellum. Total RNA was extracted from each brain region, DNase-treated, and reverse-transcribed. The cDNA obtained was analyzed by real-time polymerase chain reaction (PCR) using iNOS-specific primers (Figure 1). RNA levels were normalized to hypoxanthine guanine phosphoribosyl transferase (HPRT)-1 and fold induction was calculated by comparison to uninfected controls. Data obtained from these experiments indicate that iNOS mRNA expression was elevated in the subcortex and cerebellum of HSV-infected mice by 7 d.p.i. and remained elevated at 21 and 14 d.p.i., respectively. Interestingly, although iNOS levels in the cortex peaked at a later time point (i.e., 14 d.p.i.), increased expression was still detected at 21 d.p.i. in this region.

Kinetics of HO-1 mRNA induction

Because HO-1 induction is a widely used indicator of oxidative stress, we next investigated the kinetics of HO-1 mRNA expression throughout the course of viral brain infection. HO-1 mRNA expression levels were quantified at 1, 7, 14, and 21 d.p.i. For these experiments, cortex, subcortex, and cerebellum were harvested and total RNA was isolated and reverse-transcribed. cDNA obtained was analyzed by real-time PCR using primers specific for HO-1 (Figure 2). Transcript levels were normalized to HPRT and data are presented as fold induction over uninfected controls. Results obtained during these experiments show that, similar to the kinetics of iNOS expression, HO-1 mRNA levels were highly elevated in the subcortex and cerebellum of mice as early as 7 d.p.i. Levels in the cortex were also highest at day 14 p.i. To further confirm that the HO-1 gene was induced in the HSV-infected brain, bioluminescence imaging studies were performed using HSV-infected HO-1 promoter–luciferase transgenic mice. For these experiments, the transgenic mice were infected via the i.n. route and subsequently imaged at 3, 5, 7, and 9 d.p.i. (Figure 3A and B). Baseline levels of expression were also determined prior to infection. Data obtained from these experiments show

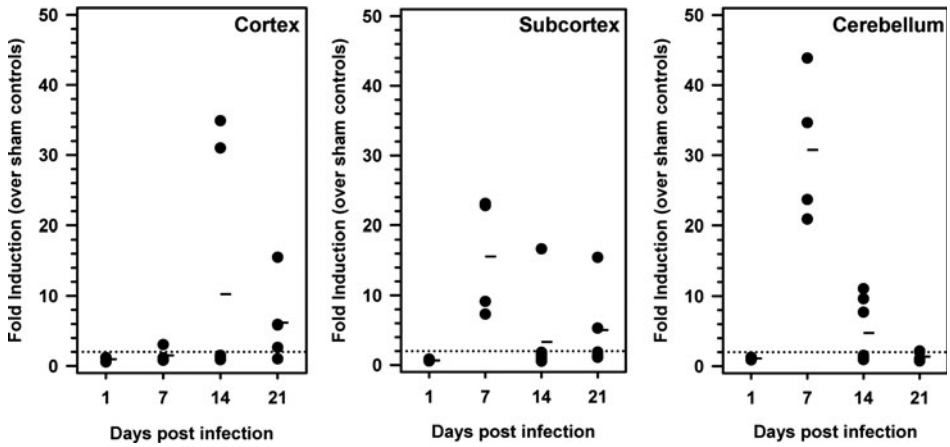

Figure 1 Kinetics of iNOS mRNA induction in the brains of animals with herpes encephalitis. BALB/c mice were intranasally infected with 2.5×10^5 PFU HSV-1 17syn+ and brain tissue was harvested at 1, 7, 14, and 21 d.p.i. The cortex, subcortex, and cerebellum were separately collected and total RNA was isolated and reverse-transcribed. Quantitative real-time PCR was performed using primers specific for iNOS. Sample variation was controlled by normalization to hypoxanthine phosphoribosyltransferase-1 (HPRT-1) and fold induction was calculated by comparison to uninfected controls. Three to five mice were sacrificed for each time point and each closed circle represents one animal. Dashes represent the mean per group at each time point.

that viral infection stimulated HO-1 promoter activity in the brains of infected animals, between 3 and 9 d.p.i.

Oxidative damage in the HSV-infected brain

To investigate the implications of oxidative stress during viral encephalitis, levels of 8-isoprostane in infected brains were quantified using ELISA (Cayman Chemical, Ann Arbor, MI). Isoprostanes are produced by the random oxidation of tissue phospholipids through free radical–catalyzed peroxidation of arachidonic acid. 8-Isoprostane, in particular, appears in tissue that has undergone oxidative degradation and is used as a marker of antioxidant deficiency and oxidative stress (Morrow *et al,* 1995; Morrow *et al*, 1990; Reilly *et al*, 1997). Brains were removed from HSV-infected animals ($n = 3$–4 mice/group) at 0, 7, 14, and 21 d.p.i. and the tissue was processed for isolation of 8-isoprostanes. This analysis revealed significantly higher 8-isoprostane levels in the brains of HSV-infected mice at 7 d.p.i. as compared to sham-infected controls; $p < .05$, Student's *t* test (Figure 4A).

HSV-induced oxidative brain damage was further confirmed using immunohistochemical staining for the presence of 8-hydroxydeoxyguanosine (8-OH-dG) and 3-nitrotyrosine. 8-OH-dG detection is a sensitive and widely used biomarker of *in vivo* oxidative damage to cellular DNA because its formation reflects a guanosine modification that occurs due to attack by hydroxyl radicals that are formed as byproducts of oxidative stress. Likewise, production of highly reactive nitrogen species derived from NO, such as peroxynitrite, leads to the nitration of tyrosine residues

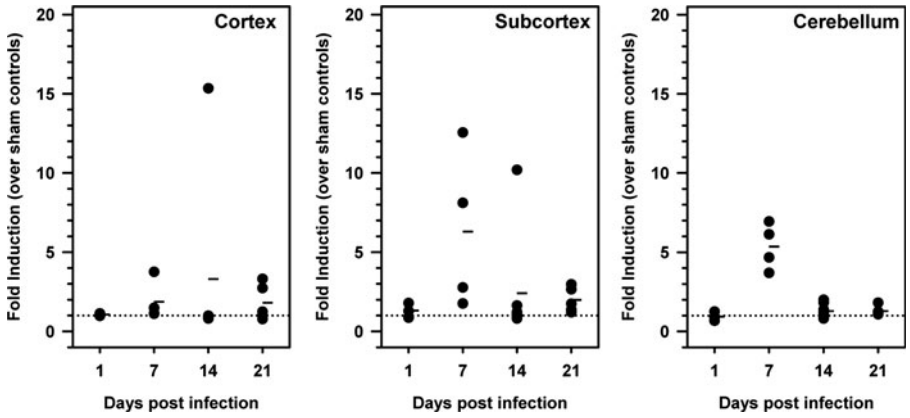

Figure 2 Kinetics of HO-1 mRNA induction in the brains of animals with herpes encephalitis. BALB/c mice were intranasally infected and brain tissue was harvested at 1, 7, 14, and 21 d.p.i. The cortex, subcortex, and cerebellum were separately collected and total RNA was isolated and reverse-transcribed. RT-qPCR was performed using primers specific for HO-1. Sample variation was controlled by normalization to HPRT-1 and fold induction was calculated by comparison to sham-infected controls. Three to five mice were sacrificed for each time point and each closed circle represents one animal. Dashes represent the mean per group at each time point.

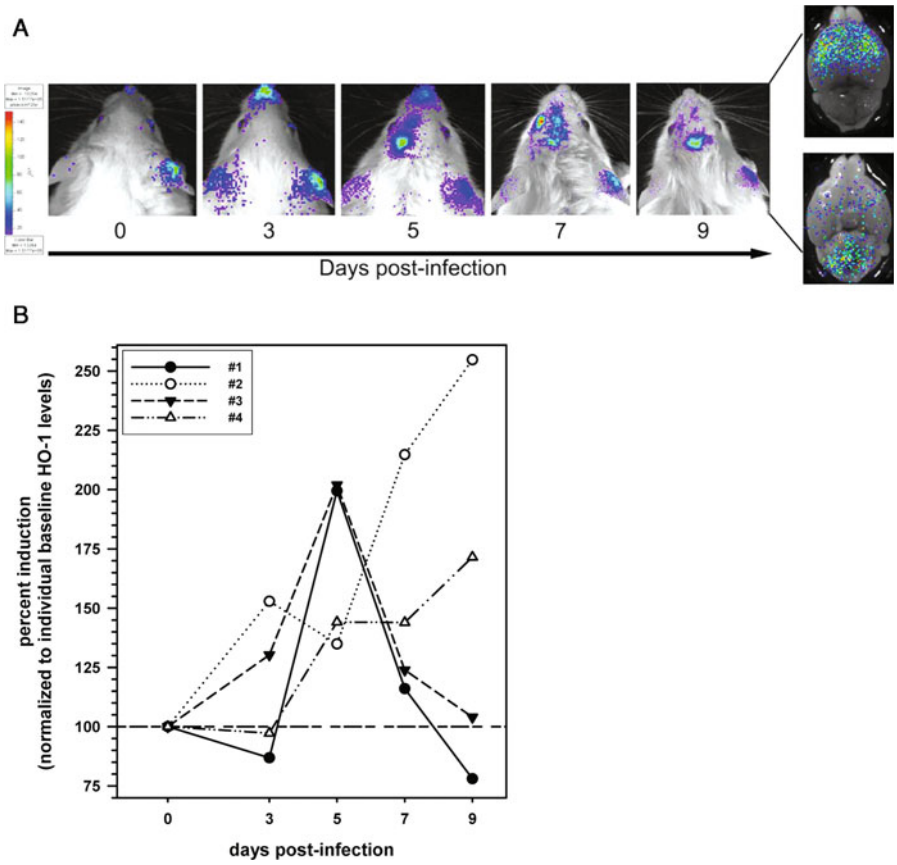

Figure 3 Bioluminescence imaging of HO-1 induction during herpes encephalitis. HO-1 promoter–luciferase expressing transgenic mice were infected via the i.n. route with 5×10^5 PFU of HSV strain 17syn+. For bioimaging, the infected animals were injected intraperitoneally with D-luciferin (a bioluminescent substrate for luciferase) and live images were acquired on a Xenogen IVIS Imaging System (Alameda, CA) 5 to 10 min after the luciferin injection. (**A**) Time course of HO-1 promoter activity in the HSV-infected murine brain: images of a representative animal are shown. Right panel insert represents direct imaging of (*top*) dorsal and (*bottom*) ventral sides of brain extracted from the skull (day 9). (**B**) Signal intensity of the HO-1 promoter–luciferase expression in the brain was quantified as photons/s/cm^2 at each indicated time point and expressed as percent induction normalized to each individual animal's ($n = 4$) baseline level (100%).

in tissue proteins. Therefore, nitrotyrosine formation indicates the presence of RNS as well as cellular damage. For these experiments, thinly sliced sections cut from frozen brain tissue obtained from HSV-infected murine brains (6 d.p.i.), along with sham-infected controls, were probed with either goat anti-8-OH-dG antiserum or anti-3-nitrotyrosine antibodies. Results from these experiments demonstrate infection-induced oxidative brain damage, as positive staining for both 8-OH-dG and nitrotyrosine were observed (Figure 4B).

CD45(int)/CD11b(+) resident microglia are the cellular source of iNOS mRNA

To identify the cellular source of iNOS, and thereby the cell type mediating oxidative injury in the virus-infected brain, leukocytes were pooled from five HSV-infected murine brains (7 d.p.i.), isolated by centrifugation on a Percoll cushion, and sorted into four distinct populations using fluorescence-activated cell sorting (FACS), with anti-mouse CD45 and CD11b antibodies (Abs) (Figure 5A). These sorted populations were then individually assayed for iNOS mRNA expression by real-time reverse transcriptase (RT)-PCR, as described for infected brain tissue. Results from these experiments indicated that the CD45^{int}/CD11b$^+$microglia were the major cellular source of iNOS during experimental murine herpes encephalitis (Figure 5B).

Discussion

Previously published studies have shown that both acute and latent HSV-1 brain infections are associated with oxidative damage. During the acute phase, HSV-infected mice developed encephalitic symptoms associated with severe inflammation, viral protein expression, and significantly elevated levels of F_4-neuroprostanes and F_2-isoprostanes, which are sensitive *in vivo* biomarkers of oxidant injury, in the brain (Milatovic *et al*, 2002). Additional studies investigating oxidative brain damage during the latent phase of herpes virus infection have demonstrated

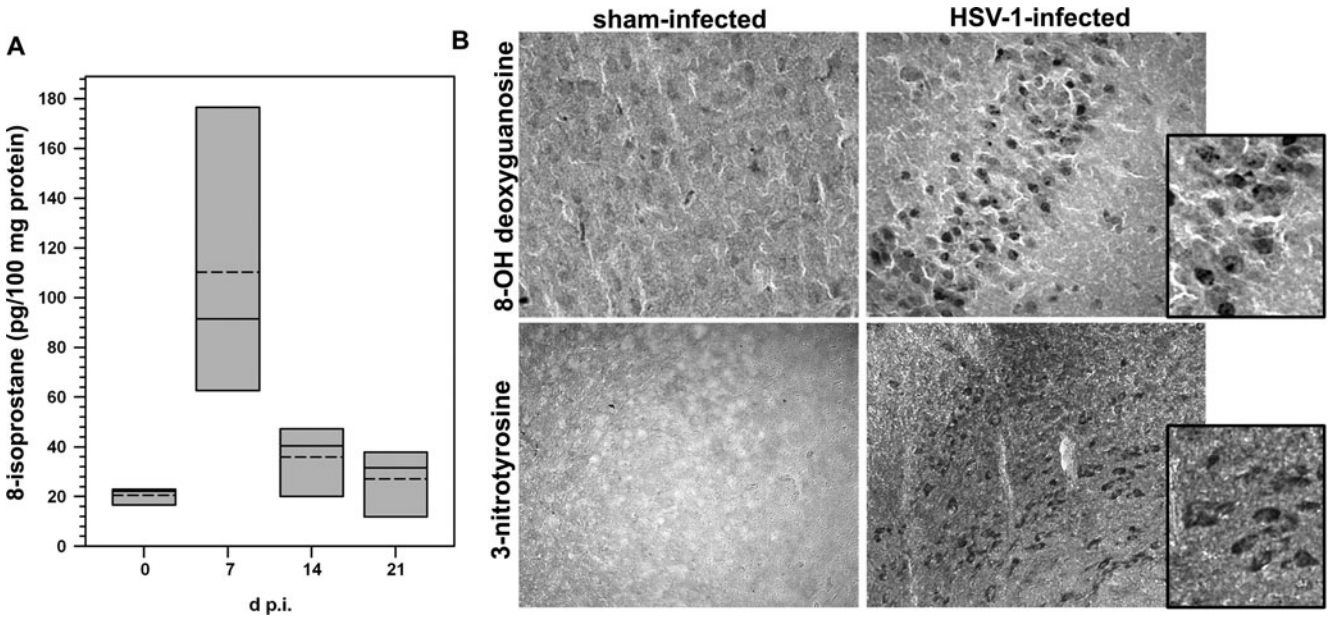

Figure 4 Infection-induced oxidative brain damage. (**A**) Quantitative assessment of lipid peroxidation in the brains of animals with herpes encephalitis using ELISA for 8-isoprostanes. Brains were removed from animals infected with HSV via the intranasal route ($n =$ 3–4 mice/group) at 0, 7, 14, and 21 d.p.i. and prepared for analysis according to the protocol provided by the manufacturer (8-Isoprostane Affinity Purification Kit; Cayman Chemicals). 8-Isoprostane levels were subsequently assessed using an ELISA (8-Isoprostane EIA Kit; Cayman) and the data are presented as box plots showing the mean (*dashed line*), median (*solid line*), and range (*shaded box*) expressed as pg/100 mg protein. Significantly higher levels of 8-isoprostane were found in the brains of HSV-infected mice at 7 d.p.i. as compared to sham-infected controls; $p < .05$, Student's t test. (**B**) Immunohistochemical staining for the products of oxidative brain damage during herpes encephalitis. Twenty-micron sections were cut from frozen brain tissues of mice collected 6 days following infection with HSV via direct intracerebral inoculation. Oxidative damage to DNA was probed using goat anti-8-OH-dG antiserum (Chemicon) in both sham-infected and HSV-infected animals. Tissues were pretreated with 10 μg/ml of proteinase K for 40 min at 37°C. Brain sections from sham-infected and HSV-infected mice were also stained with anti-3-nitrotyrosine Abs demonstrating NO-induced protein damage. For these experiments, sections of brain tissue were pretreated using heat-induced epitope retrieval. Incubation with a rabbit polyclonal anti-nitrotyrosine Ab (Chemicon) was overnight, and the reaction was developed using DAB.

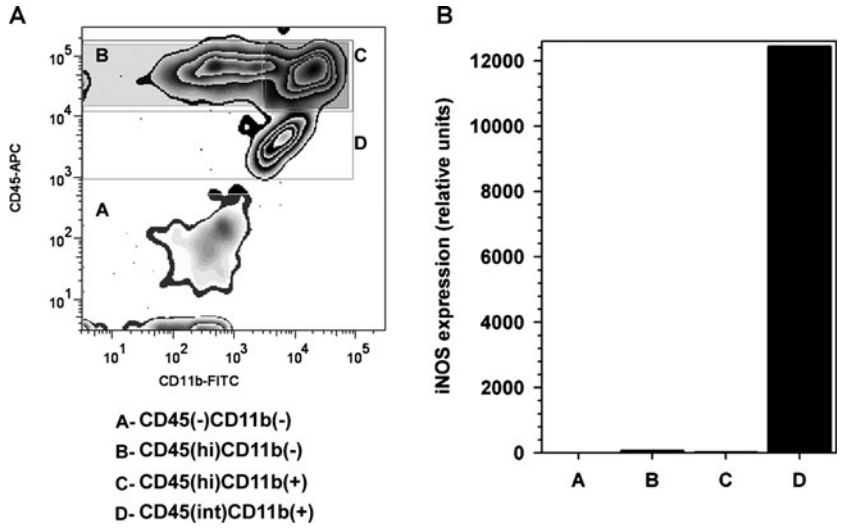

Figure 5 Expression of iNOS mRNA by CD45(int)/CD11b(+) resident microglial cells. (**A**) Single-cell suspensions of brain tissue obtained from HSV-infected mice ($n =$ 5 animals; 7 d.p.i.) were banded on a 70% Percoll cushion. Brain leukocytes at the 30% to 70% Percoll interface were collected, labeled with mouse Abs specific for CD45 and CD11b, and sorted into four populations (A through D) using FACS. (**B**) Total RNA extracted from each of the separated populations (A through D) was analyzed by real-time RT-PCR for expression of iNOS. Relative transcript levels in cells isolated from brain tissues of five animals normalized to HPRT expression are presented.

the presence of 8-hydroxyguanosine immunoreactivity, indicative of hydroxyl radical attack on RNA or DNA, a result that suggests that inflammatory mediators could be responsible for damage found in the absence of HSV proteins (Valyi-Nagy *et al*, 2000). Recently, it has been shown *in vitro* that HSV infection increases reactive oxygen species in neural cell cultures as early as 1 h p.i. and these levels remain elevated at 24 h p.i. (Kavouras *et al*, 2007). Results reported in this paper show that microglial cells are the major source of iNOS produced in the brain during herpes encephalitis. Although there is little doubt that oxidative mediators are produced to protect the brain and control viral infection, *in vivo* evidence presented here suggests an additional consequence of this innate neuroimmune response: infection-induced RNS formation and oxidative damage within the virus-infected brain. The presence of oxidative mediators in the HSV-infected brain was further corroborated by the detection of HO-1 mRNA, as HO-1 expression is known to be a sensitive marker of oxidative stress (Chen and Regan, 2007).

Comparisons between the kinetics of HSV-induced neuroimmune responses and those of mortality in our murine encephalitis model are especially intriguing. In this model, experimentally infected mice typically succumb to infection between 7 and 10 d.p.i. We have previously described a robust microglia-driven cascade of proinflammatory neuroimmune responses that peaks at this time (Marques *et al*, 2006). Although the effect of oxidative stress in the brain on the survival of the host cannot be assessed from the present study, this damage was observed at the same time HSV infection–induced mortality began. In any event, the results of this study further emphasize the important role of microglial cells during the progression of herpes encephalitis.

Although microglial activation is necessary for host defense, the activated state of this cell type has also been linked to neurotoxicity, neurodegeneration, and chronic neuroinflammation in several disorders including Alzheimer's disease, Parkinson's disease, amyotrophic lateral sclerosis, and human immunodeficiency virus (HIV)-associated dementia (Reynolds *et al*, 2007a). In the case of HSV brain infection, microglia are not only a source of proinflammatory cytokines and chemokines, such as tumor necrosis factor (TNF)-α, interleukin (IL)-1β, and CXCL10 (Lokensgard *et al*, 2001; Marques *et al*, 2006), but also, as we describe here, a major source of NO. Recent studies investigating interactions between NO and cytokines in the murine brain demonstrate that NO together with TNF-α is a critical combination that leads to intense neurodegeneration and demyelination *in vivo* (Blais and Rivest, 2004). In support of this notion, results from another study investigating the effects of macrophage depletion on the pathogenesis of HSV hepatitis suggest that overproduction of free radicals in combination with cytokines, such as TNF-α, IL-6, and interferon (IFN)-α may result in hepatic cell apoptosis (Irie and Shiga, 2005). The connection between HSV infection and oxidative stress is especially interesting because it has been recently reported that infection increases ROS in cultured neuronal cells and that this induction is actually required for efficient viral replication (Kavouras *et al*, 2007). The authors suggest that lipid-peroxidation by-products generated in infected neuronal cells may be important regulators of HSV pathogenesis in the brain. Such collateral evidence indicates that in addition to suppressing aberrant proinflammatory cytokine and chemokine production, along with immune cell infiltration; regulating oxidative stress in the infected brain may be important in controlling the severity and long-term sequelae following herpes encephalitis.

A recent report regarding the protective effects of regulatory T cells (Tregs) on toxicity-induced neuronal loss, in an experimental murine model of Parkinson's disease, showed that Tregs mediated neuroprotection through suppression of microglial oxidative stress and inflammation (Reynolds *et al*, 2007b). Another study investigating the effects of glucorticoid treatment on progression of herpes encephalitis in mice revealed that the timing of treatment is critical to survival. These experiments revealed that anti-inflammatory treatment concomitant with viral infection exacerbated the disease, whereas the same treatment began at 3 d.p.i. significantly improved survival and was associated with decreased neurodegeneration (Sergerie *et al*, 2007). The authors suggested that by restraining inflammation and limiting microglial activation, glucocorticoids could decrease cerebral damage and increase survival, thereby protecting the host from fatal disease. Potential benefits of anti-inflammatory therapy in herpes encephalitis treatment are further supported by a recent clinical case report describing remarkable improvement as a result of high-dose steroid therapy in a case of severely progressive herpes encephalitis, despite appropriate course of antiviral medication and decreased viral load (Musallam *et al*, 2007).

It is also interesting to consider how modulating the production of HO-1 may benefit the central nervous system (CNS). It has previously been reported that up-regulation of HO-1 mRNA paralleled the time profile of viral replication and iNOS expression in HSV-1–infected rat brains (Fujii *et al*, 1999). In addition to being well known as a marker for oxidative stress, HO-1 is also regarded as a potent cytoprotective, anti-inflammatory stress response gene. Mounting evidence suggests that HO-1 induction protects both vascular cells and astrocytes from oxidative injury (Chen-Roetling *et al*, 2005; Ono *et al*, 2002; Regan *et al*, 2000). HO-1 has been shown to mediate its anti-inflammatory effects by targeting p38α mitogen-activated protein kinase (MAPK) for degradation (Silva *et al*, 2006). This is particularly relevant to viral-microglial interactions, as we have previously shown that HSV-induced cytokine and

chemokine production from human microglial cells is dependent on the p38 MAPK pathway (Lokensgard *et al*, 2001). The full range of anti-inflammatory effects of HO-1 in the brain remains to be determined, and these studies may elucidate new targets for therapeutic treatment of diseases induced by activated microglia.

Materials and methods

Virus and infection
HSV-1 strain 17syn$^+$ was propagated and titrated using plaque assay on rabbit skin fibroblasts (CCL68; American Type Culture Collection, Manassas, VA). Eight- to 10-week-old BALB/c female mice (Charles River Laboratories, Boston, MA) were anesthetized and infected via the i.n. route with 1.25×10^5 HSV-1 plaque-forming units (PFU)/nostril (2.5×10^5 PFU/mouse). Experiments assessing oxidative damage by immunochemical staining used 8- to 10-week BALB/c female mice that were anesthetized and given an intracerebral (i.c.) injection of 1×10^4 PFU/mouse of sucrose-purified HSV-1 17 syn$^+$ into the left cerebral hemisphere. Control animals were inoculated with vehicle solution (saline). Bioluminescent imaging experiments were performed with i.n. infected (5×10^5 PFU/mouse) FVB HO-1-*luc* Xen mice (Taconic Farms, Germantown, NY). This light producing animal model carries a mouse *HO-1–luciferase* fusion containing a 15-kb mouse HO-1 promoter and modified firefly luciferase cDNA (Promega pGL-3), (Zhang *et al*, 1999, 2001, 2002).

Isolation of brain leukocytes and sorting using FACS
Leukocytes were isolated from HSV-infected murine brains using a previously described procedure with minor modifications (Ford *et al*, 1995; Marten *et al*, 2003). Briefly, brain tissues harvested from 4–6 animals were minced finely in RPMI (2 g/L D-glucose and 10 mM HEPES) and digested in 0.25% trypsin (Ca/Mg-free Hanks' balanced salt solution [HBSS]) at room temperature for 20 min. The single-cell suspension was resuspended in 30% Percoll and banded on a 70% Percoll cushion at $900 \times g$ at 15°C. For sorting, brain leukocytes obtained from the 30% to 70% Percoll interface were stained with anti-mouse CD45-Allophycocyanin (APC) (eBioscience, San Diego, CA) and anti-mouse CD11b-FITC for 45 min at 4°C. Nonoverlapping populations were separated using a fluorescence-activated cell sorter (FACS; BD FACSAria, BD Biosciences). Total RNA, isolated from the sorted cell populations, was analyzed by real-time RT-PCR for iNOS expression.

Assessment of iNOS and HO-1 mRNA expression
Upon sacrifice, murine brains were dissected into three regions: cortex, subcortex, and cerebellum to elucidate any regional differences in mRNA expression of oxidative and anti-oxidative enzyme mRNA. Total RNA was extracted from brain tissue homogenates using the TRIzol Reagent (Invitrogen, Carlsbad, CA) according to the manufacturer's instructions. cDNA was synthesized using 1 to 5 μg of total RNA, SuperScript II reverse transcriptase (Invitrogen Life Technologies, Carlsbad, CA) and oligo dT_{6-12}primers (Sigma-Genosys, The Woodlands, TX). Quantitative real-time PCR was performed using the FullVelocity SYBR Green QPCR master mix (Stratagene, La Jolla, CA) following the manufacturer's specifications. The 25-μl final reaction volume consisted of premade reaction mix (SYBR Green I dye, reaction buffer, Taq DNA polymerase, and dNTPs), 0.3 mM of each primer, and 0.5 ng cDNA in water. Reaction conditions for PCR for the Mx3000P QPCR System (Stratagene) were as follows: polymerase activation at 95°C for 5 min, 40 denaturation cycles of 95°C for 10 s, and annealing/elongation at 60°C for 30 s. Primers used in the amplification of iNOS and HO-1 were designed from the murine genes (GenBank accession nos. NM_010927, 5′-TGGCCACCTTGTTCAGCTACG-3′ and 5′-GCCAAGGCCAAACACAGCATA-3′, 211-bp product, and NM_010442, 5′-CACGCATATACCCGCTACCT-3′ and 5′-CCAGAGTGTTCATTCGAGCA-3′, 176-bp product, respectively). Primers recognizing the housekeeping gene, hypoxanthine guanine phosphoribosyl transferase (HPRT)-1 were designed from the murine HPRT mRNA sequence (GenBank accession no. NM_013556, 5′-TGCTCGAGA TGTCATGAAGG-3′ and 5′-AATCCAGCAGGTCAG CAAAG-3′, 294-bp product). A melting curve analysis was performed to assess primer specificity and product quality by denaturation at 95°C, annealing at 55°C, and melting at a rate of 0.1°C/s to 95°C. The relative levels of PCR product were quantified using the $2(-\Delta\Delta C_T)$ method (Livak and Schmittgen, 2001).

Quantitative assessment of lipid peroxidation
Brains from sham- or HSV-infected mice were quickly harvested, weighed and homogenized in 1 ml of ice-cold 0.1 M phosphate buffer (pH 7.4) containing 1 mM EDTA and 10 μM indomethacin for 30 s. An equal volume of 15% KOH was added to the homogenized mixture and incubated at 40°C for 60 min, followed by the addition of 2 ml 100% ethanol containing 0.01% butylated hydroxytoluene (BHT). After vortexing, the mixture was incubated for 5 min at 4°C and centrifuged at 1500 rpm for 10 min (4°C). The supernatants were then diluted with 2 ml 0.1 M phosphate buffer containing 0.5 M NaCl and 0.05% sodium azide. Each sample was purified by passage through an 8-isoprostane affinity sorbent column (Cayman, Ann Arbor, MI). The purified samples were then subjected to vacuum centrifugation until lyophilized (about 4 h). The lyophilized samples were reconstituted with enzyme immunoassay buffer (50 μl) and reaction buffer (50 μl containing 8-isoprostane antiserum and tracer), and added to 96-well plate for 8-isoprostane assay (Cayman). The

plate was incubated at room temperature for 18 h followed by washing (5×, 3 min each) with washing buffer. One hundred microliters of Ellman's reagent was added and the plate was shaken in the dark for 90 to 120 min. The plate was read at 405 nm using a microplate reader (Molecular Devices, Sunnyvale, CA) and the corrected sample and standard optical density was calculated according to the manufacturer's protocol. The final total 8-isoprostane concentrations were normalized to each sample's total protein concentration and expressed as pg/mg protein.

Immunohistochemical staining for oxidative brain damage

Immunohistochemical staining was performed using a previously described protocol (Lokensgard et al, 1999; Marques et al, 2006). Briefly, sham- or HSV-infected mice were sacrificed and perfused with 2% sodium nitrate and phosphate-buffered saline (PBS), followed by 4% paraformaldehyde. Murine brains were harvested, submerged in 4% paraformaldehyde for 24 h, and transferred to a 30% sucrose solution for 2 days. Infected brains were then cryosectioned (20 μm) and stained for (1) oxidative damage to DNA using goat anti-8-hydroxyoxyguanosine (8-OH-dG) antiserum (Chemicon-Millipore, Billerica, MA); and (2) cellular damage induced by reactive nitrogen species using rabbit anti-nitrotyrosine antibody (Chemicon-Millipore). Murine brain sections were either pre-treated with 10 μg/ml proteinase K (Invitrogen, Carlsbad, CA) for 40 min at 37°C (for 8-OH-dG staining) or subjected to heat-induced epitope retrieval (for nitrotyrosine staining) according to manufacturer's protocol. After washing (3×, 5 min each) with Tris-buffered saline (TBS), slides were incubated in blocking solution (TBS containing 1% bovine serum albumin [BSA], 0.05% triton X-100, and 10% serum: normal rabbit serum (for 8-OH-dG) or goat serum (for nitrotyrosine) for 60 min. After washing, the slides were incubated overnight at 4°C with each primary antibody (Ab) diluted in blocking solution (anti-8-OH-dG serum, 1:200; anti- nitrotyrosine, 1:500). After washing (4×, 5 min each), slides were incubated in biontinylated secondary antibodies (for 8-OH-dG: rabbit anti-goat antibody, 1:200; for nitrotyrosine: goat anti-rabbit antibody, 1:200) for 60 min. After washing (4×, 5 min each), the slides were incubated for 60 min in Vectastain ABC reagents diluted according to the manufacturer's protocol. After washing (4×, 5 min each), the bound complex was visualized by incubating the slides in 0.05% 3,3′-diaminobenzidine (DAB) and 0.03% hydrogen peroxide for 5 to 10 min at room temperature. Color development was terminated by washing and slides were visualized and analyzed using light microscopy.

Bioluminescence imaging

HO-1 promoter activity was assessed in the brains of i.n. infected (5×10^5 PFU) HO-1–luciferase transgenic mice (Malstrom *et al*, 2004; Zhang *et al*, 1999, 2001, 2002). Imaging of firefly luciferase in mice was performed on a charge-coupled device camera (Xenogen, Alameda, CA) as previously described with minor modifications (Luker *et al*, 2003). Briefly, 150 μg (100 μl) of D-luciferin (a bioluminescent substrate for luciferase; Gold Biotechnology, St. Louis, MO) was administered to anesthetized mice by intraperitoneal injection. The anesthetic cocktail was a combination of ketamine (100 mg/ml) and xylazine (16 mg/ml); 50 μl/mouse was injected i.p. and the anesthetic effects lasted approximately 20 min. Imaging began 5 min after administration of D-luciferin. Images were acquired for 5 min. Signal intensity of luciferase expression, measured by the amount of transmitted light, was represented as a pseudocolor image ranging from violet (least intense) to red (most intense). Corresponding gray-scale photographs and color luciferase images were superimposed and photon levels were quantified as photons/sec/cm^2 from the cranial region of the mouse with LivingImage (Xenogen) and Igor (Wavemetrics, Lake Oswego, OR) image analysis software. Data are reported as individual values from four mice at different time points p.i. as described in the figure legends. No animals died as a result of imaging or chemical treatment.

References

Adler H, Beland JL, Del-Pan NC, Kobzik L, Brewer JP, Martin TR, Rimm IJ (1997). Suppression of herpes simplex virus type 1 (HSV-1)-induced pneumonia in mice by inhibition of inducible nitric oxide synthase (iNOS, NOS2). *J Exp Med* **185:** 1533–1540.

Baranano DE, Snyder SH (2001). Neural roles for heme oxygenase: contrasts to nitric oxide synthase. *Proc Natl Acad Sci U S A* **98:** 10996–1002.

Blais V, Rivest S (2004). Effects of TNF-alpha and IFN-gamma on nitric oxide-induced neurotoxicity in the mouse brain. *J Immunol* **172:** 7043–7052.

Bredt DS, Snyder SH (1992). Nitric oxide, a novel neuronal messenger. *Neuron* **8:** 3–11.

Chen M, Regan RF (2007). Time course of increased heme oxygenase activity and expression after experimental intracerebral hemorrhage: correlation with oxidative injury. *J Neurochem* **103:** 2015–2021.

Chen-Roetling J, Benvenisti-Zarom L, Regan RF (2005). Cultured astrocytes from heme oxygenase-1 knockout mice are more vulnerable to heme-mediated oxidative injury. *J Neurosci Res* **82:** 802–810.

Chora AA, Fontoura P, Cunha A, Pais TF, Cardoso S, Ho PP, Lee LY, Sobel RA, Steinman L, Soares MP (2007). Heme oxygenase-1 and carbon monoxide suppress autoimmune neuroinflammation. *J Clin Invest* **117:** 438–447.

Croen KD (1993). Evidence for antiviral effect of nitric oxide. Inhibition of herpes simplex virus type 1 replication. *J Clin Invest* **91:** 2446–2452.

Ford AL, Goodsall AL, Hickey WF, Sedgwick JD (1995). Normal adult ramified microglia separated from other central nervous system macrophages by flow cytometric sorting. Phenotypic differences defined and direct ex vivo antigen presentation to myelin basic protein-reactive CD4+ T cells compared. *J Immunol* **154:** 4309–4321.

Fujii S, Akaike T, Maeda H (1999). Role of nitric oxide in pathogenesis of herpes simplex virus encephalitis in rats. *Virology* **256:** 203–212.

Gamba G, Cavalieri H, Courreges MC, Massouh EJ, Benencia F (2004). Early inhibition of nitric oxide production increases HSV-1 intranasal infection. *J Med Virol* **73:** 313–322.

Garthwaite J (1991). Glutamate, nitric oxide and cell-cell signalling in the nervous system. *Trends Neurosci* **14:** 60–67.

Irie H, Shiga J (2005). Pathogenesis of herpes simplex hepatitis in macrophage-depleted mice: possible involvement of tumor necrosis factor-alpha and inducible nitric oxide synthase in massive apoptosis. *Anat Sci Int* **80:** 199–211.

Kavouras JH, Prandovszky E, Valyi-Nagy K, Kovacs SK, Tiwari V, Kovacs M, Shukla D, Valyi-Nagy T (2007). Herpes simplex virus type 1 infection induces oxidative stress and the release of bioactive lipid peroxidation by-products in mouse P19N neural cell cultures. *J NeuroVirol* **13:** 416–425.

Livak KJ, Schmittgen TD (2001). Analysis of relative gene expression data using real-time quantitative PCR and the 2(-Delta Delta C(T)) Method. *Methods* **25:** 402–408.

Lokensgard JR, Hu S, Sheng W, vanOijen M, Cox D, Cheeran MC, Peterson PK (2001). Robust expression of TNF-alpha, IL-1beta, RANTES, and IP-10 by human microglial cells during nonproductive infection with herpes simplex virus. *J NeuroVirol* **7:** 208–219.

Luker GD, Prior JL, Song J, Pica CM, Leib DA (2003). Bioluminescence imaging reveals systemic dissemination of herpes simplex virus type 1 in the absence of interferon receptors. *J Virol* **77:** 11082–11093.

MacLean A, Wei XQ, Huang FP, Al-Alem UA, Chan WL, Liew FY (1998). Mice lacking inducible nitric-oxide synthase are more susceptible to herpes simplex virus infection despite enhanced Th1 cell responses. *J Gen Virol* **79(Pt 4):** 825–830.

Malstrom SE, Jekic-McMullen D, Sambucetti L, Ang A, Reeves R, Purchio AF, Contag PR, West DB (2004). In vivo bioluminescent monitoring of chemical toxicity using heme oxygenase-luciferase transgenic mice. *Toxicol Appl Pharmacol* **200:** 219–228.

Marques CP, Hu S, Sheng W, Cheeran MC, Cox D, Lokensgard JR (2004). Interleukin-10 attenuates production of HSV-induced inflammatory mediators by human microglia. *Glia* **47:** 358–366.

Marques CP, Hu S, Sheng W, Lokensgard JR (2006). Microglial cells initiate vigorous yet non-protective immune responses during HSV-1 brain infection. *Virus Res* **121:** 1–10.

Marten NW, Stohlman SA, Zhou J, Bergmann CC (2003). Kinetics of virus-specific CD8+ T-cell expansion and trafficking following central nervous system infection. *J Virol* **77:** 2775–2778.

Martin LD, Krunkosky TM, Dye JA, Fischer BM, Jiang NF, Rochelle LG, Akley NJ, Dreher KL, Adler KB (1997). The role of reactive oxygen and nitrogen species in the response of airway epithelium to particulates. *Environ Health Perspect* **105(Suppl 5):** 1301–1307.

Milatovic D, Zhang Y, Olson SJ, Montine KS, Roberts LJ 2nd, Morrow JD, Montine TJ, Dermody TS, Valyi-Nagy T (2002). Herpes simplex virus type 1 encephalitis is associated with elevated levels of F2-isoprostanes and F4-neuroprostanes. *J NeuroVirol* **8:** 295–305.

Moncada S, Palmer RM, Higgs EA (1991). Nitric oxide: physiology, pathophysiology, and pharmacology. *Pharmacol Rev* **43:** 109–142.

Morrow JD, Frei B, Longmire AW, Gaziano JM, Lynch SM, Shyr Y, Strauss WE, Oates JA, Roberts LJ 2nd (1995). Increase in circulating products of lipid peroxidation (F2-isoprostanes) in smokers. Smoking as a cause of oxidative damage. *N Engl J Med* **332:** 1198–1203.

Morrow JD, Hill KE, Burk RF, Nammour TM, Badr KF, Roberts LJ, 2nd (1990). A series of prostaglandin F2-like compounds are produced in vivo in humans by a non-cyclooxygenase, free radical-catalyzed mechanism. *Proc Natl Acad Sci U S A* **87:** 9383–9387.

Musallam B, Matoth I, Wolf DG, Engelhard D, Averbuch D (2007). Steroids for deteriorating herpes simplex virus encephalitis. *Pediatr Neurol* **37:** 229–232.

Nathan CF, Hibbs JB Jr (1991). Role of nitric oxide synthesis in macrophage antimicrobial activity. *Curr Opin Immunol* **3:** 65–70.

Ono S, Komuro T, Macdonald RL (2002). Heme oxygenase-1 gene therapy for prevention of vasospasm in rats. *J Neurosurg* **96:** 1094–1102.

Regan RF, Guo Y, Kumar N (2000). Heme oxygenase-1 induction protects murine cortical astrocytes from hemoglobin toxicity. *Neurosci Lett* **282:** 1–4.

Reilly MP, Delanty N, Roy L, Rokach J, Callaghan PO, Crean P, Lawson JA, FitzGerald GA (1997). Increased formation of the isoprostanes IPF2alpha-I and 8-epi-prostaglandin F2alpha in acute coronary angioplasty: evidence for oxidant stress during coronary reperfusion in humans. *Circulation* **96:** 3314–3320.

Reynolds A, Laurie C, Mosley RL, Gendelman HE (2007a). Oxidative stress and the pathogenesis of neurodegenerative disorders. *Int Rev Neurobiol* **82:** 297–325.

Reynolds AD, Banerjee R, Liu J, Gendelman HE, Mosley RL (2007b). Neuroprotective activities of CD4+CD25+ regulatory T cells in an animal model of Parkinson's disease. *J Leukoc Biol* **82:** 1083–1094.

Sato K, Balla J, Otterbein L, Smith RN, Brouard S, Lin Y, Csizmadia E, Sevigny J, Robson SC, Vercellotti G, Choi AM, Bach FH, Soares MP (2001). Carbon monoxide generated by heme oxygenase-1 suppresses the rejection of mouse-to-rat cardiac transplants. *J Immunol* **166:** 4185–4194.

Sergerie Y, Boivin G, Gosselin D, Rivest S (2007). Delayed but not early glucocorticoid treatment protects the host during experimental herpes simplex virus encephalitis in mice. *J Infect Dis* **195:** 817–825.

Silva G, Cunha A, Gregoire IP, Seldon MP, Soares MP (2006). The antiapoptotic effect of heme oxygenase-1 in endothelial cells involves the degradation of p38 alpha MAPK isoform. *J Immunol* **177:** 1894–1903.

Turcanu V, Dhouib M, Poindron P (1998a). Heme oxygenase inhibits nitric oxide synthase by degrading heme: a negative feedback regulation mechanism for

nitric oxide production. *Transplant Proc* **30:** 4184–4185.

Turcanu V, Dhouib M, Poindron P (1998b). Nitric oxide synthase inhibition by haem oxygenase decreases macrophage nitric-oxide-dependent cytotoxicity: a negative feedback mechanism for the regulation of nitric oxide production. *Res Immunol* **149:** 741–744.

Valyi-Nagy T, Olson SJ, Valyi-Nagy K, Montine TJ, Dermody TS (2000). Herpes simplex virus type 1 latency in the murine nervous system is associated with oxidative damage to neurons. *Virology* **278:** 309–321.

Zhang W, Contag PR, Hardy J, Zhao H, Vreman HJ, Hajdena-Dawson M, Wong RJ, Stevenson DK, Contag CH (2002). Selection of potential therapeutics based on in vivo spatiotemporal transcription patterns of heme oxygenase-1. *J Mol Med* **80:** 655–664.

Zhang W, Contag PR, Madan A, Stevenson DK, Contag CH (1999). Bioluminescence for biological sensing in living mammals. *Adv Exp Med Biol* **471:** 775–784.

Zhang W, Feng JQ, Harris SE, Contag PR, Stevenson DK, Contag CH (2001). Rapid in vivo functional analysis of transgenes in mice using whole body imaging of luciferase expression. *Transgenic Res* **10:** 423–434.